Tunable Nd, La:SrF_2 laser and passively Q-switched operation based on gold nanobipyramids saturable absorber*

Feng Zhang(张峰)[1,2], Hua-Nian Zhang(张华年)[1,2], Dan-Hua Liu(刘丹华)[1,†], Jie Liu(刘杰)[1,2,‡], Feng-Kai Ma(马凤凯)[3], Da-Peng Jiang(姜大朋)[3], Si-Yuan Pang(逄思远)[3], Liang-Bi Su(苏良碧)[3], and Jun Xu(徐军)[4]

[1] *Shandong Provincial Key Laboratory of Optics and Photonic Device, School of Physics and Electronics, Shandong Normal University, Jinan* 250014, *China*
[2] *Institute of Data Science and Technology, Shandong Normal University, Jinan* 250014, *China*
[3] *Synthetic Single Crystal Research Center, Shanghai Institute of Ceramics, Chinese Academy of Sciences, Shanghai* 201800, *China*
[4] *Key Laboratory of Transparent and Opto-functional Inorganic Materials, Shanghai Institute of Ceramics, Chinese Academy of Sciences, Shanghai* 201800, *China*

(Received 13 July 2016; revised manuscript received 18 September 2016; published online 20 December 2016)

A novel Nd, La:SrF_2 disordered crystal is prepared, and its continuous-wave wavelength tuning operation is performed for the first time. Employing a surface plasmon resonance (SPR) based gold nanobipyramids (G-NBPs) saturable absorber, we obtain a compact diode-pumped passively Q-switched Nd, La:SrF_2 laser. The stable Q-switched pulse operates with the shortest pulse duration of 1.15 μs and the maximum repetition rate of 41 kHz. The corresponding single pulse energy is 2.24 μJ. The results indicate that G-NBPs could be a promising saturable absorber applied to the diode-pumped solid state lasers (DPSSLs).

Keywords: tunable laser, Q-switching, Nd, La:SrF_2 crystal, gold nanobipyramids

PACS: 42.55.–f, 42.55.Xi, 42.60.Gd, 42.60.Fc **DOI:** 10.1088/1674-1056/26/2/024205

1. Introduction

Passively Q-switched solid state lasers have advantages in the aspects of compactness, simplicity and low cost in design compared with those using the active technique such as electro–optic and acousto–optic modulators. Two key factors affect the passively Q-switched laser performances, the laser crystal and the saturable absorbers. Recently, Nd-doped disordered crystals have attracted a great deal of attention as four-level operation, low output threshold, broad absorption and fluorescence spectra. Particularly, the AeF_2–LnF_3–NdF_3 (*Ae*: Sr^{2+}, Ca^{2+}, Ba^{2+}; *Ln*: Y^{3+}, Lu^{3+}, La^{3+}, Gd^{3+}) disordered crystal have performed excellent laser outputs.[1–11] Codoping the buffer ions (Y^{3+}, Lu^{3+}, La^{3+}, Gd^{3+}) could alleviate the detrimental concentration quenching effect and improve the laser performances markedly. Besides, the disordered lattice structure causes the absorption and fluorescence spectra to inhomogeneously broaden, which is beneficial to generating ultrashort pulse. In 2013, Doualan *et al.* demonstrated the continuous wave laser performance of Nd:CaF_2 crystals by codoping with Y^{3+} and Lu^{3+} buffer ions.[4] In 2014, Qin *et al.* demonstrated 103 fs mode-locked pulses by a gain linewidth-variable Nd,Y:CaF_2 disordered crystal.[9] In 2016, Zhang *et al.* demonstrated 992-mW continuous wave and dual-wavelength passively mode locked operation based on an Nd,Gd:SrF_2 disordered crystal.[11]

For the other part, nano-materials, especially two-dimensional nano-materials, have received considerable attention for their wide-band saturable absorption property applied to the pulse laser generation.[12–24] As an important component of nano-materials, metal nano-materials have attracted enormous attention, mainly due to the large third order nonlinearity, broadband absorption and fast response time on a time scale of a few picoseconds.[25–32] For example, gold-nano material has a large third-order nonlinear coefficient ($\sim 10^{-6}$ esu) when compared with the traditional nano-materials (e.g., carbon nanotube (10^{-8} esu$\sim 10^{-9}$ esu) and graphene ($\sim 10^{-7}$ esu)),[33,34] making it easy to obtain self-starting Q-switched or mode-locked operation as an SA. The saturable absorption property of gold-nano materials is governed by the excitation of localized surface plasmon resonance (SPR).[35] As a typical gold-nano material, gold nanorods have two SPR bands, a strong longitudinal SPR (LSPR) band and a weak transverse SPR (TSPR) band. By changing the aspect ratio of the nanorods, we can turn the LSPR bands from the visible to the near-infrared wavelength region. Based on gold nanorods, Kang *et al.* demonstrated Yb-, Er-, and Tm-doped pulsed fiber lasers by controlling the SPR peak at the emission wavelength region of the dope ions such as 1030, 1550, and 1950 nm, indicated in Refs. [36]–[39]. Recently, Fan *et al.* reported a passively Q-switched erbium-doped fiber laser

*Project supported by the National Natural Science Foundation of China (Grant Nos. 61475089, 51432007, and 61422511).
†Corresponding author. E-mail: danhua_liu@126.com
‡Corresponding author. E-mail: jieliu@sdnu.edu.cn
© 2017 Chinese Physical Society and IOP Publishing Ltd

by using evanescent field interaction with a gold-nanosphere based on an SA.[39]

The SPR properties of G-NBPs are similar to those of the gold nanorods. The strong LSPR band can be tuned by changing the draw ratio of the G-NBPs. Compared with a gold nanorod, G-NBP might have good performances of being used as SA, due to its strong resonance absorption peak at the tip. In 2016, Zhang and Liu demonstrated a diode-pumped passively Q-switched solid state laser based on the gold nanobipyramids SA.[40]

In this paper, we investigate a novel Nd, La:SrF_2 disordered crystal and obtain its wavelength tuning operation for the first time. Employing a gold nanobipyramid SA, we also obtain passively Q-switched operation. The shortest pulse width is 1.15 μs, and the corresponding single pulse energy is 2.24 μJ. As a fast response SA, G-NBP has a promising prospect of application to the ultrashort pulse generation.

2. Nd,La:SrF_2 tunable laser

Nd,La:SrF_2disordered crystal is a typical AeF_2–LnF_3–NdF_3-(*Ae*: Sr^{2+}, Ca^{2+}, Ba^{2+}; *Ln*: Y^{3+}, Lu^{3+}, La^{3+}, Gd^{3+}), type crystal. Codoping La^{3+} can increase its lattice disorder and give rise to the fluorescence spectrum inhomogeneously broadened. In the experiment, A "V"-type resonator is employed to generate the continuous wave operation as shown in Fig. 1. The pump source is a fiber-coupled laser diode (LD) which emitted light beams at 795 nm, and that matches well with the absorption peak of Nd,La:SrF_2 crystal. The coupling fiber has a core diameter of 105 μm and a numerical aperture (NA) of 0.22. The pump light is delivered into the Nd,La:SrF_2 crystal through a 1:2 coupling focusing system. Doped with 0.5% at Nd^{3+} and 8% at La^{3+}, the SrF_2 disordered crystal had three dimensions of 3 mm×3 mm×5 mm. Input flat mirror M1 was anti-reflection coated for the pump light and high reflection coated at 1030 nm∼1080 nm. Concave mirror M2 has a radius of curvature of 200 mm and is high reflection coated at 1030 nm∼1080 nm. The flat output mirror M3 has a transmittance of 3%. Continuous wave (CW) operation with a maximum output power of 992 mW is obtained. Then an SF 10 dispersion prism is inserted into the L2 arm. By adjusting the angle of the output coupler, a total tuning range of 24.1 nm from 1046.7 nm to 1070.8 nm is performed. Moreover, the tuning curve from 1051.9 nm to 1064.3 nm is smooth, indicating that it is possible for Nd,La:SrF_2 disordered crystal to generate a 100 fs mode locked pulse. Figure 2 shows the wavelength tuning spectrum of Nd,La:SrF_2 laser and fluorescence spectrum of Nd,La:SrF_2 crystal.

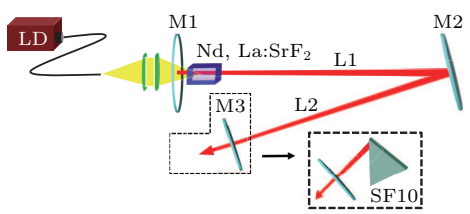


Fig. 1. (color online) Schematic diagram of the Nd,La:SrF_2 wavelength tuning laser.

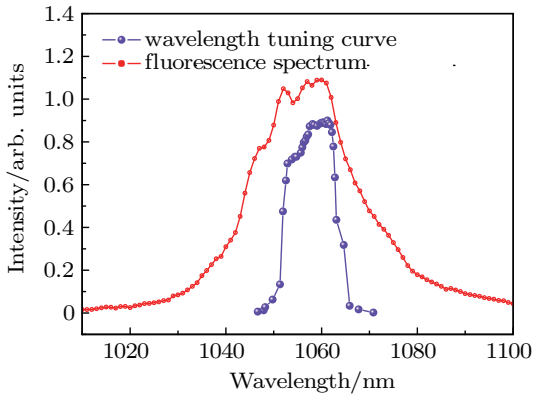


Fig. 2. (color online) Fluorescence spectrum of Nd,La:SrF_2 crystal and wavelength tuning curve of Nd,La:SrF_2 crystal laser.

3. Passively Q-switched operation based on gold nanobipyramid SA

3.1. Preparation of the gold nanobipyramids SA

The employed G-NBPs in our experiment are synthesized through a seed-mediated growth method, which is prepared with 50 μL of 20-mM chloroauric acid and 74 μL of 1% trisodium citrate added into 9.87-mL pure water, which is vigorously stirred for 1 min. After the solution is in a long-standing status after 150 μL of 0.01-M ice, $NaBH_4$ is added and vigorously stirred for 1 min. The growth solution is prepared with 28.5 mL of 0.01-M cetyltributylammonium bromide, 1.2 mL of 0.01-M gold chloride acid, 60 μL of 0.01-M $AgNO_3$, and 0.4 mL of 0.1-M ascorbic acid, which are dissolved in a flask. After a 75-μL seed solution has been injected into the growth solution, the mixed solution is centrifuged at a rate of 6000 rpm for 10 min and placed into the oven with a temperature of 65 °C for 10 h. Figure 3(a) shows the gold nanobipyramids solution. The G-NBP dispersion was in a long-term stable state. The final G-NBP SA film is formed by casting the dispersion onto a flat substrate and then followed by slow drying at room temperature.

Figure 3(b) shows the transmission electron microscopy (TEM) images of the G-NBPs SA film with a scale bar of 200 nm. The corresponding absorption spectrum of the gold nanobipyramids is also shown in Fig. 3(c). As depicted, there are two absorption peaks for the G-NBPs. The transverse SPR absorption peak is nearly located at 555 nm. Additionally, the longitudinal SPR absorption peak is 1092 nm. At 1060 nm, the G-NBP has strong SPR absorption. So the demonstration of a passively Q-switched Nd, La:SrF_2 laser operating at 1060 nm is suitable for verifying the absorption properties of the G-NBP SA. The saturable absorption of the G-NBP was measured by a home-made mode-locked Nd,La:SrF_2 solid state

laser based on SESAM. The laser emitted ∼ 2-ps stable mode locked pulse at 1061 nm with a repetition of 81.5 MHz. By changing the incident fluence, the reflectivities of G-NBPs increase in a range from 75% to 88%. The measurement shows that the G-NBP has a modulation depth of 13% and saturation fluence of 1 μJ/cm^2 at 1.06 μm as shown in Fig. 3(d).

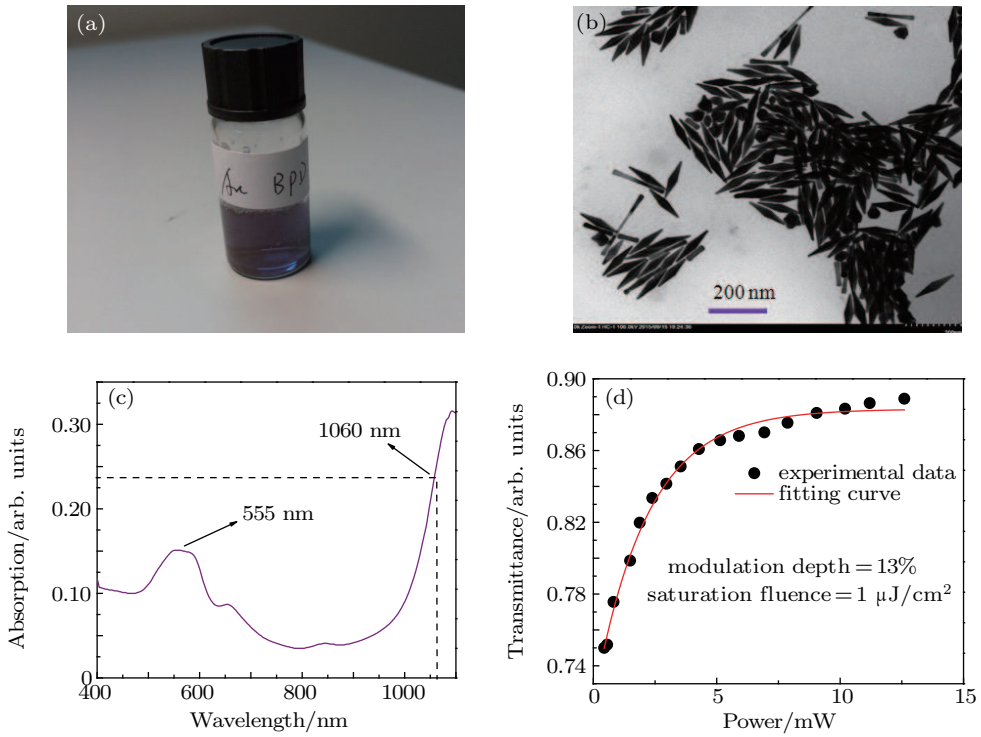


Fig. 3. (color online) (a) Gold nanobipyramid solution. (b) TEM images of the gold nanobipyramid film. (c) Absorption coefficient versus wavelength. (d) Nonlinear absorption of the gold nanobipyramid film.

3.2. Passively Q-switched operation

Schematic diagram of passively Q-switched Nd,La:SrF$_2$ laser based on G-NBP SA is shown in Fig. 4. A standard concave-plano resonator with a total length of 33 mm is employed to generate the Q-switched pulse. The input concave mirror M1 has an 80 mm radius of curvature (anti-reflection coated for the pump light and high reflection coated at 1030 nm∼1080 nm). The pump source and coupling focusing system are the same as those in the laser tuning operation. Firstly, continuous-wave operation with a maximum output of 323 mW is generated from the laser cavity. After inserting the transmission-type G-NBPs SA near the output mirror, and slightly adjusting the position and the angle of the G-NBP SA, stable Q-switched operation is realized. Figure 5 shows the output powers versus the absorbed pump power of Nd,La:SrF$_2$ laser under CW and Q-switched operation.

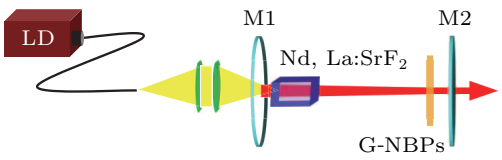


Fig. 4. (color online) Schematic diagram of passively Q-switched Nd,La:SrF$_2$ laser based on G-NBP SA.

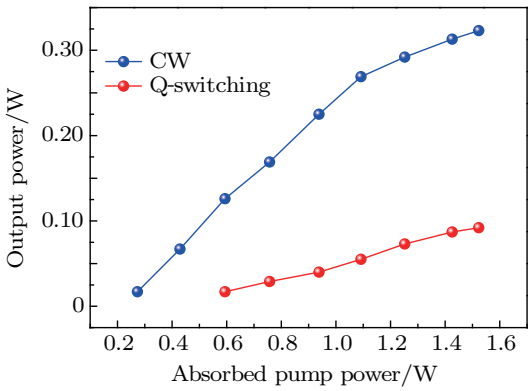


Fig. 5. (color online) Output powers of Nd,La:SrF$_2$ laser versus the absorbed pump power under continuous wave and Q-switched operation.

The output laser spectra are recorded by an optical spectrum analyzer (Avaspec-3648, USB2.) and are shown in Fig. 6(a). As we can see, the Q-switched spectrum peaked at 1060 nm, and is 1.2-nm shorter than the continuous wave spectrum. Otherwise, the full width at half maximum (FWHM) of the spectrum is narrowed compared with the CW operation. With the absorbed pump power increased from 0.594 W to 1.523 W, stable Q-switching is realized. The repetition rate increases from 29 kHz to 41 kHz, and pulse width decreases from 2.05 μs to 1.15 μs, respectively (Fig. 6(b)). Employing a high-speed detector (EOT, ET-3000, rise time < 175 ps) and

a 1-GHz-bandwidth oscilloscope (Tektronix-DPO4104), the pulse train is measured and shown in Fig. 6(c). The beam quality is measured by a commercial M^2 factor analyzer (Spiricon-m2-200s-usb) in the highest output level when pump power is 1.523 W. The results show $M_x^2 = 1.8$ and $M_y^2 = 2.1$ in x and y directions perpendicular to the propagation axis (Fig. 6(d)).

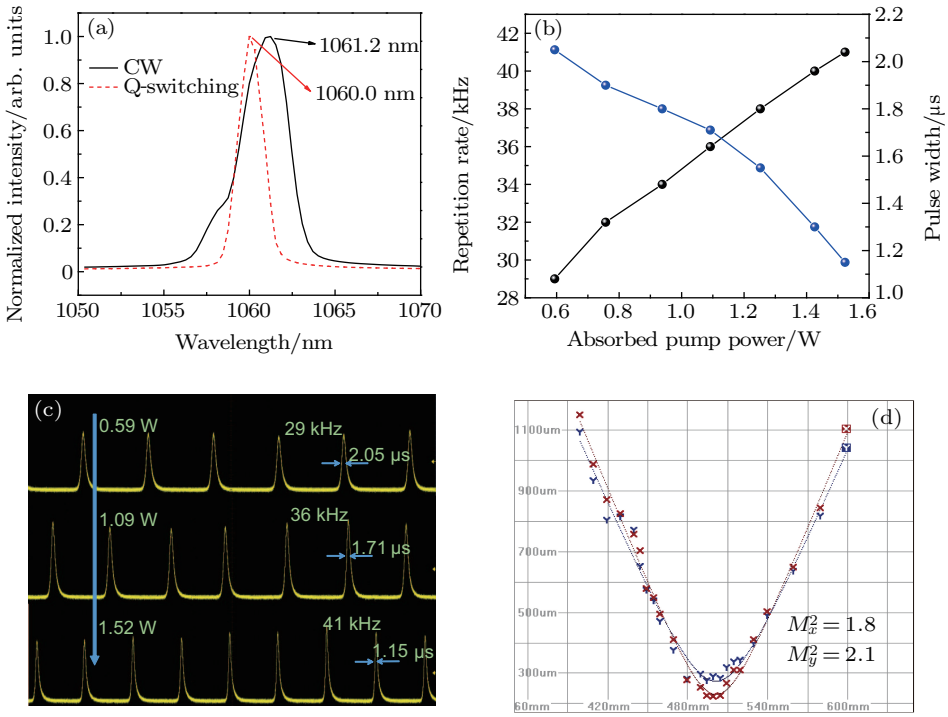


Fig. 6. (color online) (a) Output spectra of the Nd,La:SrF_2 disordered crystal under continuous wave and Q-switched operation. (b) Repetition rate and pulse width versus absorbed pump power. (c) Pulse trains versus the absorbed pump power on a time scale of 20 μs. (d) The beam quality of passively Q-switched Nd,La:SrF_2 laser.

4. Conclusions

In this work, we experimentally demonstrate a diode pumped passively Q-switched Nd, La:SrF_2 laser based on a gold nanobipyramids saturable absorber. Stable Q-switched laser with a shortest pulse duration of 1.15 μs and corresponding maximum repetition rate of 41 kHz is obtained. The calculated maximum single pulse energy is 2.24 μJ. As the parameters of the G-NBP are further optimized and the laser resonator changes, CW mode-locked operation can be expected.

References

[1] Liu J, Fan M W, Su L B, Jiang D P, Ma F K, Zhang Q and Xu J 2014 *Laser Phys.* **24** 035802

[2] Kaminskii A A, Bohat'y L, Becker P, Eichler H J and Rhee H 2007 *Laser Phys. Lett.* **4** 668

[3] Zhu J F, Zhang L J, Gao Z Y, Wang J L, Wang Z H, Su L B, Zheng L H, Wang J Y, Xu J and Wei Z Y 2015 *Laser Phys. Lett.* **12** 035801

[4] Doualan J L, Su L B, Brasse G, Benayad A, Ménard V, Zhan Y Y, Braud A, Camy P, Xu J and Moncorgé R 2013 *J. Opt. Soc. Am. B* **30** 3018

[5] Su L B, Wang Q G, Li H J, Brasse G, Camy P, Doualan J L, Braud A, Moncorgé R, Zhan Y Y, Zheng L H, Qian X B and Xu J 2013 *Laser Phys. Lett.* **10** 035804

[6] Jelínek M, Kubeček V, Su L B, Jiang D P, Ma F K, Zhang Q, Cao Y X and Xu J 2014 *Laser Phys. Lett.* **11** 055001

[7] Zhang Q, Su L B, Jiang D P, Ma F K, Qin Z P, Xie G Q, Zheng J G, Deng Q H, Zheng W G, Qian L J and Xu J 2015 *Chin. Opt. Lett.* **13** 071402

[8] Qin Z P, Xie G Q, Ma J, Ge W Y, Yuan P, Qian L J, Su L B, Jiang D P, Ma F K, Zhang Q, Cao Y X and Xu J 2014 *Opt. Lett.* **39** 1737

[9] Wei L, Han H N, Tian W L, Liu J X, Wang Z H, Zhu Z, Jia Y L, Su L B, Xu J and Wei Z Y 2014 *Appl. Phys. Express* **7** 092704

[10] Zhang F, Fan X W, Liu J, Ma F K, Jiang D P, Pang S Y, Su L B, Xu J 2016 *Opt. Mater. Express* **6** 1513

[11] Bao Q, Zhang H, Wang Y, Ni Z, Yan Y, Shen Z X, Loh K P and Tang D Y 2009 *Adv. Funct. Mater.* **19** 3077

[12] Luo Z, Zhou M, Weng J, Huang G, Xu H, Ye C and Cai Z 2010 *Opt. Lett.* **35** 3709

[13] Li H P, Xia H D, Wang Z G, Zhang X X, Chen Y F, Zhang S J, Tang X G and Liu Y 2014 *Chin. Phys. B* **23** 024209

[14] Baek I H, Lee H W, Bae S, Hong B H, Ahn Y H, Yeom D I and Rotermund F 2012 *Appl. Phys. Express* **5** 032701

[15] Sun Z, Hasan T, Torrisi F, Popa D, Privitera G, Wang F, Bonaccorso F and Basko D M 2010 *ACS Nano* **4** 803

[16] Sotor J, Sobon G and Abramski K M 2014 *Opt. Express* **22** 13244

[17] Luo Z C, Liu M, Liu H, Zheng X W, Luo A P, Zhao C J, Zhang H, Wen S C, and Xu W C 2013 *Opt. Lett.* **38** 5212

[18] Liu J H, Tian J R, Hu M T, Xu R Q, Dou Z Y, Yu Z H and Song Y R 2015 *Chin. Phys. B* **24** 024215

[19] Lin Y H, Chi Y C and Lin G R 2013 *Laser Phys. Lett.* **10** 055105

[20] Wang S, Yu H, Zhang H, Wang A, Zhao M, Chen Y, Mei L and Wang J 2014 *Adv. Mater.* **26** 3538

[21] Zhu J F, Wang X L, He B R, *et al.* 2015 *Chin. Phys. B* **24** 097601

[22] Mao D, Wang Y, Ma C, Han L, Jiang B, Gan X, Hua S, Zhang W, Mei T and Zhao J 2015 *Sci. Rep.* **5** 7965

[23] Zhao C, Zou Y, Chen Y, Wang Z, Lu S, Zhang H, Wen S and Tang D Y 2012 *Opt. Express* **20** 27888

[24] Elim H I, Yang J, Lee J Y, Mi J and Ji W 2006 *Appl. Phys. Lett.* **88** 083107

[25] Jiang T, Xu Y, Tian Q J, Liu L, Kang Z, Yang R Y, Qin G S and Qin W P 2012 *Appl. Phys. Lett.* **101** 151122

[26] Kim K H, Griebner U and Herrmann J 2012 *Opt. Lett.* **37** 1490

[27] Kim K H, Griebner U and Herrmann J 2012 *Opt. Express* **20** 16174
[28] Kang Z, Xu Y, Zhang L, Jia Z X, Liu L, Zhao D, Feng Y, Qin G S and Qin W P 2013 *Appl. Phys. Lett.* **103** 041105
[29] Kang Z, Guo X Y, Jia Z X, Xu Y, Liu L, Zhao D, Qin G S and Qin W P 2013 *Opt. Mater. Express* **3** 1986
[30] Kang Z, Gao X J, Zhang L, Feng Y, Qin G S and Qin W P 2015 *Opt. Mater. Express* **5** 794
[31] Wang X D, Luo Z C, Liu H, Liu M, Luo A P and Xu W C 2014 *Appl. Phys. Lett.* **105** 161107
[32] Liao H B, Xiao R F, Fu J S, Yu P, Wong G K L and Sheng P 1997 *Appl. Phys. Lett.* **70** 1
[33] Yamashita S 2012 *J. Lightwave Technol.* **30** 427
[34] Zhang T H, Ying M R, Fang Z Y, Yang H D, *et al.* 2005 *Physics* **34** 0 (in Chinese)
[35] Kang Z, Xu Y, Zhang L, Jia Z, Liu L, Zhao D and Qin W 2013 *Appl. Phys. Lett.* **103** 041105
[36] Jiang T, Xu Y, Tian Q, Liu L, Kang Z, Yang R and Qin W 2012 *Appl. Phys. Lett.* **101** 151122
[37] Kang Z, Guo X, Jia Z, Xu Y, Liu L, Zhao D and Qin W P 2013 *Opt. Mater. Express* **3** 1986
[38] Kang Z, Li Q, Gao X J, Zhang L, Jia Z X, Feng Y and Qin W P 2014 *Laser Phys. Lett.* **11** 035102
[39] Fan D F, Mou C, Bai X, Wang S, Chen N and Zeng X 2014 *Opt. Express* **22** 18537
[40] Zhang H N and Liu J 2016 *Opt. Lett.* **41** 1150